2mi4

NASA TECHNICAL MEMORANDUM

NASA TM X-71530

NASA TM X-71530

EVIDENCE OF CHARGE EXCHANGE PUMPING IN CALCIUM-XENON SYSTEM

by Donald L. Chubb
Lewis Research Center
Cleveland, Ohio 44135

TECHNICAL PAPER presented at
Twenty-sixth Annual Gaseous Electronics Conference
sponsored by the American Physical Society
Madison, Wisconsin, October 16-19, 1973

EVIDENCE OF CHARGE EXCHANGE PUMPING IN CALCIUM-XENON SYSTEM

by Donald L. Chubb

Lewis Research Center

SUMMARY

Charge exchange between xenon ions and calcium atoms may produce an inversion between the 5s or 4d and 4p energy levels of the calcium ions. A low power flowing xenon plasma seeded with calcium was utilized to determine if charge exchange or electron collisions populate the 5s and 4d levels of Ca^+. Line intensity ratios proportional to the density ratios n_{5s}/n_{4p} and n_{4d}/n_{4p} were measured. From the dependence of these intensity ratios on power input to the xenon plasma it was concluded that charge exchange pumping of the 5s and 4d levels predominates over electron collisional pumping of these levels. Also, by comparing intensity ratios obtained using argon and krypton in place of xenon with those obtained in xenon the same conclusion was made.

E-7932

INTRODUCTION

Earlier it was proposed[1] that charge exchange between xenon ions and calcium atoms may produce an inversion between two of the energy levels of the calcium ions. The near-resonance charge exchange reaction is described by the following relation:

$$Xe^+ + Ca \rightarrow Xe + Ca_u^+ + \Delta E$$

where $\Delta E = I_{Xe} - (I_{Ca} + E_{Ca_u^+})$ is the energy defect, I and E are ionization and excitation potentials, respectively, and Ca_u^+ is the proposed upper laser level. If Ca_u^+ is the $5s^2S_{1/2}$ level as assumed in reference 1, then $\Delta E = -0.451$ eV. From the adiabatic theory of Massey[2] (also discussion in ref. 3) the maximum cross section for charge exchange occurs at the following relative velocity between the colliding ion and atom:

$$v_{max} = \frac{A|\Delta E|}{h}$$

where h is the Planck constant and A is the adiabatic parameter, which has been found to have a mean value of about 0.7 nm (ref. 3). Using $\Delta E = -0.451$ eV we find $v_{max} \approx 7.6\times10^6$ cm/sec. For velocities below this the charge exchange cross section decreases as $e^{-1/v}$ (ref. 3).

In the experiment to be described here $v < 7.6\times10^6$ cm/sec. Therefore, the rear resonance charge exchange cross section may be expected to be small, although no experimental verification is available. However,

Melius[4] has pointed out that charge exchange may also result from so-called "curve crossing" of the potential energy curves of the molecular complexes $(Xe^+ - Ca)$ and $(Xe - Ca_u^+)$. He points out that charge exchange may occur by "curve crossing" between $Xe^+(^2P_{1/2})$ (which is a metastable state 1.3 eV above the $^2P_{3/2}$ ground state) and Ca to produce $Ca^+(4d^2D_{3/2}$ or $4d^2D_{5/2})$ or $Ca^+(5s^2S_{1/2})$:

$$Xe^+\left(^2P_{1/2}\right) + Ca \rightarrow Xe + Ca^+\left(4d^2D_{3/2} \text{ or } 4d^2D_{5/2}\right) + 0.276 \text{ eV}$$

$$Xe^+\left(^2P_{1/2}\right) + Ca \rightarrow Xe + Ca^+\left(5s^2S_{1/2}\right) + 0.855 \text{ eV}$$

Curve crossing cannot play a role in charge exchange between ground state $Xe^+(^2P_{3/2})$ and Ca since $\Delta E < 0$. In this case the potential energy curve of $(Ca - Xe^+(^2P_{3/2}))$ always lies below the $(Xe - Ca^+(5s^2S_{1/2}))$ potential energy curve. In reference 5 curve crossing theory was applied to the cadmium-helium and magnesium-neon systems. They found fairly good agreement between the theoretical cross sections and cross sections deduced from experimental relative intensity data. Their experiment utilized a flowing plasma in much the same way as the experiment described in this report.

The experimental set-up is shown in figure 1. A steady state flowing xenon plasma is produced by a low power (~100 watts) MPD arc.[6] Calcium is injected into the plasma beam where charge exchange occurs between xenon ions and calcium atoms. Relative intensity and plasma electron temperature measurements were made. From these data and some theoretical expressions it is possible to determine if charge exchange or electron collisional excitation is responsible for populating the proposed upper laser levels (5s and 4d levels of Ca^+). However, it is not possible to distinguish between a near resonance or a "curve crossing" charge exchange.

THEORY

Level Continuity Equations

Figure 2 shows an energy level diagram of the calcium ion. Also shown are the relevant wavelengths, λ_{ij}, and transition probabilities, A_{ij}, obtained from reference 8. We will consider the possibility of populating both the 5s and 4d levels by charge exchange with xenon ions in the ground state $^2P_{3/2}$ or metastable xenon ions in the $^2P_{1/2}$ state. For the moment, however, ignore the specific collisional mechanisms that populate the Ca^+ levels and denote the net population rate for the i^{th} level by W_i. Assume the flowing system in figure 1 can be represented by a quasi-one dimensional model. If stimulated emission is neglected and all Ca^+ states have the same velocity, v, then the continuity equations for the Ca^+ levels shown in figure 2 are the following:

for the $4p^2P_{1/2}$ level density, n_2:

$$\frac{dn_2}{dt} \equiv \frac{\partial n_2}{\partial t} + \frac{1}{A}\frac{\partial(An_2\ v)}{\partial x} = W_2 + n_4A_{41} + n_5A_{51} - \frac{n_2}{\tau_2} \tag{1}$$

for the $4p^2P_{3/2}$ level density, n_3:

$$\frac{dn_3}{dt} \equiv \frac{\partial n_3}{\partial t} + \frac{1}{A}\frac{\partial(An_3\ v)}{\partial x} = W_3 + n_4A_{43} + n_5A_{53} + n_6A_{63} - \frac{n_3}{\tau_3} \tag{2}$$

for the $5s^2S_{1/2}$ level density, n_4:

$$\frac{dn_4}{dt} \equiv \frac{\partial n_4}{\partial t} + \frac{1}{A}\frac{\partial(An_4\ v)}{\partial x} = W_4 - n_4(A_{42} + A_{43}) \tag{3}$$

for the $4d^2D_{3/2}$ level density, n_5:

$$\frac{dn_5}{dt} \equiv \frac{\partial n_5}{\partial t} + \frac{1}{A}\frac{\partial(An_5\ v)}{\partial x} = W_5 - n_5(A_{52} + A_{53}) \tag{4}$$

for the $4d^2D_{5/2}$ level density, n_6:

$$\frac{dn_6}{dt} \equiv \frac{\partial n_6}{\partial t} + \frac{1}{A}\frac{\partial(An_6\ v)}{\partial x} = W_6 - n_6A_{63} \tag{5}$$

The τ's denote lifetimes of a Ca^+ level.

The quantity A is the cross sectional area of the flow at station x. The flow part of the continuity equations (the $\frac{1}{A}\frac{\partial(Anv)}{\partial x}$ terms), will be proportional to L/v, where L is the characteristic length of the flow. For the experiment described here $v \sim 10^6$ cm/sec and $L \sim 1$ cm. Therefore, the characteristic flow time is the order of 10^{-6} sec. The time dependent part of the continuity equation (the $\partial n/\partial t$ term) is proportional to $1/T$, where T is the characteristic time for the radiative and collisional excitation processes. Therefore, $T \sim 10^{-8}$ sec. As a result, $(v/L)T \sim 10^{-2}$ and the flow part of the continuity equations can be neglected.

Also, since the two $4p$ levels are so close in energy we assume they are in equilibrium. Therefore, for the $4p$ levels,

$$n_\ell \equiv n_2 = \frac{g_2}{g_3} n_3 \exp\left[-\frac{q(E_3 - E_2)}{kT_e}\right] \tag{6}$$

Since $(E_3 - E_2) \to 0$, we neglect the exponential term, so that

$$n_\ell \equiv n_2 = \frac{g_2}{g_3} n_3 \tag{7}$$

The g quantities denote statistical weights.

Even though the 4d levels are very close in energy we do not consider them to be in equilibrium due to experimental results to be discussed later.

If we now add equations (1) and (2) neglecting the flow terms and use equation (7) the following is obtained.

$$\omega_\ell \frac{dn_\ell}{dt} = W_\ell + n_4 A_{4\ell} + n_5 A_{5\ell} + n_6 A_{63} - \frac{n_\ell}{\tau_\ell} \tag{8}$$

Terms appearing in equation (8) are defined as follows.

$$\omega_\ell \equiv 1 + \frac{g_3}{g_2} \tag{9a}$$

$$A_{4\ell} \equiv A_{42} + A_{43} \tag{9b}$$

$$A_{5\ell} \equiv A_{52} + A_{53} \tag{9c}$$

$$\frac{1}{\tau_\ell} \equiv \frac{1}{\tau_2} + \frac{g_2}{g_3}\left(\frac{1}{\tau_3}\right) \tag{9d}$$

$$W_\ell \equiv W_2 + W_3 \tag{9e}$$

Neglecting the flow terms in equations (3) to (5) the following is obtained.

$$\frac{dn_4}{dt} = W_4 - n_4 A_{4\ell} \tag{10}$$

$$\frac{dn_5}{dt} = W_5 - n_5 A_{5\ell} \tag{11}$$

$$\frac{dn_6}{dt} = W_6 - n_6 A_{63} \tag{12}$$

The system of equations to be solved are given by (8), (10) to (12). Consider the steady state solution (d/dt = 0) of these equations.

$$n_\ell = \tau_\ell (W_\ell + n_4 A_{4\ell} + n_5 A_{5\ell} + n_6 A_{63}) \tag{13}$$

$$n_4 = \frac{W_4}{A_{4\ell}} \tag{14}$$

$$n_5 = \frac{W_5}{A_{5\ell}} \tag{15a}$$

$$n_6 = \frac{W_6}{A_{63}} \tag{15b}$$

Substituting equations (14) and (15) in (13) yields the following.

$$n_\ell = \tau_\ell (W_\ell + W_4 + W_5 + W_6) \tag{16}$$

Equation (16) states that, for steady state conditions, the density of the proposed lower laser level ($4p^2P_{1/2}$ or $4p^2P_{3/2}$) is the sum of the net pumping rates for the proposed upper laser levels ($5s^2S_{1/2}$, $4d^2D_{3/2}$, and $4d^2D_{5/2}$) and lower laser level multiplied by the lifetime of the lower laser level. Since it is desirable to have the lower laser level density as small as possible, equation (16) shows it is obviously a disadvantage to have two possible upper laser levels terminate on the same lower level.

In the discussion to follow we will be interested in the ratios n_4/n_ℓ, n_5/n_ℓ, n_6/n_ℓ, n_5/n_4, and n_6/n_5. Therefore, using equations (14) to (16) we obtain the following results.

$$\frac{n_4}{n_\ell} = \frac{W_4}{A_{4\ell}\tau_\ell (W_\ell + W_4 + W_5 + W_6)} \tag{17a}$$

$$\frac{n_5}{n_\ell} = \frac{W_5}{A_{5\ell}\tau_\ell (W_\ell + W_4 + W_5 + W_6)} \tag{17b}$$

$$\frac{n_6}{n_\ell} = \frac{W_6}{A_{63}\tau_\ell(W_\ell + W_4 + W_5 + W_6)} \tag{17c}$$

$$\frac{n_5}{n_4} = \frac{A_{4\ell}}{A_{5\ell}}\frac{W_5}{W_6} \tag{18a}$$

$$\frac{n_6}{n_5} = \frac{A_{5\ell}}{A_{63}}\frac{W_6}{W_5} \tag{18b}$$

Intensity Ratios

To determine if charge exchange is populating the proposed upper laser levels we must relate the experimental relative intensity measurements to the level densities. The monochromator detects the radiation emitted from some volume of the Ca - Xe plasma. At some particular wavelength, λ_{ij}, neglecting stimulated emission, the power of the radiation is given by the following expression:

$$\phi_{ij} = \int_{\mathscr{V}} \frac{hc}{\lambda_{ij}} n_i A_{ij}\, d\mathscr{V} = \frac{hc}{\lambda_{ij}} A_{ij} \int_{\mathscr{V}} n_i\, d\mathscr{V} \tag{19}$$

where h is Planck's constant, c is the speed of light, $\mathscr{V}$ is the volume of plasma observed by the monochromator, i denotes the level where the transition begins and j denotes the level where it terminates. The density of level i is denoted by n_i and A_{ij} is the transition probability for the $i \rightarrow j$ transition.

Experimentally we determined ratios of the intensities. Therefore, from equation (17) we obtain the following.

$$R^{\lambda_{pq}}_{\lambda_{ij}} \equiv \frac{\phi_{pq}}{\phi_{ij}} = \frac{\lambda_{ij}A_{pq}}{\lambda_{pq}A_{ij}} \frac{\int_{\mathscr{V}} n_p\, d\mathscr{V}}{\int_{\mathscr{V}} n_i\, d\mathscr{V}} \tag{20}$$

In order to remove the integral terms in equation (20) we assume the level densities are uniform over the volume, $\mathscr{V}$. This may be a questionable assumption since the monochromator detected radiation over a large fraction of the plasma. However, it should not detract from any conclusion about charge exchange pumping of the proposed upper laser levels predominating over electron collisional pumping of those levels. Since only the plasma near the Ca injection will display charge exchange all the plasma detected by the monochromator outside this region will probably be dominated by electron collision pumping. Therefore, assuming n_p and n_i

are uniform over η, equation (20) yields the following:

$$R^{\lambda_{pq}}_{\lambda_{ij}} = \frac{\lambda_{ij} A_{pq}}{\lambda_{pq} A_{ij}} \left(\frac{n_p}{n_i}\right) \tag{21}$$

Now substitute equations (17) and (18) in equation (21) and also use equations (6) and (7) and the statistical weights, wavelengths, and transition probabilities shown in figure 2.

$$R^{3706}_{3968} = \left(\frac{3968}{3706}\right)\left(\frac{0.84}{1.46}\right) \frac{n_4}{n_\ell} = 0.616 \frac{n_4}{n_\ell} \tag{22}$$

$$R^{3737}_{3934} = \left(\frac{3934}{3737}\right)\left(\frac{1.65}{1.50}\right)\left(\frac{g_2}{g_3}\right) \frac{n_4}{n_\ell} = 0.579 \frac{n_4}{n_\ell} \tag{23}$$

$$R^{3159}_{3968} = \left(\frac{3968}{3159}\right)\left(\frac{3.05}{1.46}\right) \frac{n_5}{n_\ell} = 2.62 \frac{n_5}{n_\ell} \tag{24}$$

$$R^{3179}_{3934} = \left(\frac{3934}{3179}\right)\left(\frac{3.59}{1.50}\right)\left(\frac{g_2}{g_3}\right) \frac{n_6}{n_\ell} = 1.48 \frac{n_6}{n_\ell} \tag{25}$$

$$R^{3159}_{3706} = \left(\frac{3706}{3159}\right)\left(\frac{3.05}{0.84}\right) \frac{n_5}{n_4} = 4.26 \frac{n_5}{n_4} \tag{26}$$

$$R^{3179}_{3159} = \left(\frac{3159}{3179}\right)\left(\frac{3.59}{3.05}\right) \frac{n_6}{n_5} = 1.17 \frac{n_6}{n_5} \tag{27}$$

Equations (22) to (27) give the intensity ratios in terms of the level density ratios. The density ratios are given in terms of the net pumping rates by equations (17) and (18).

To relate the density and intensity ratios to measurable plasma properties (electron temperature and density) the pumping rates must be expressed in terms of the plasma properties. There are two possible collisional pumping mechanisms for the 5s and 4d proposed upper laser levels. Both electron collisions and charge exchange with Xe^+ can produce these levels. However, for the 4p levels only electron collisional pumping will be important. Electron collisions between any of the many Ca and Ca^+ levels can produce Ca^+ in the 5s, 4p, or 4d state. However, because of the large energy difference between Ca atom states and these states of Ca^+ we neglect the production of 5s, 4p, or 4d states resulting from electron-Ca atom collisions. Also, since the Ca^+ ground state density, n_1, is much greater than the density of any of the excited Ca^+ states we assume that all electron collisional pumping of these levels results from electron-Ca^+ ground state collisions. Therefore, for the 5s level,

$$W_4 = \left(n_0 n_{Xe^+} L_0^4 - n_4 n_{Xe} K_4^o\right) + \left(n_e n_1 S_1^4 - n_e n_4 U_4^1\right) \tag{28}$$

The first term in brackets is the net production rate resulting from charge exchange and the second term in brackets is the net production rate resulting from electron-Ca^+ ground state collisions. The term L_0^4 is the charge exchange excitation rate, S_1^4 is the electron collisional excitation rate, while K_4^o and U_4^1 are the corresponding deexcitation rates. The density n_{Xe^+} denotes either the Xe^+ ($^2P_{3/2}$) ground state density or the Xe^+ ($^2P_{1/2}$) metastable density and n_0 is the density of ground state Ca..

Since we expect $n_0 n_{Xe^+} >> n_4 n_{Xe}$ and $n_1 >> n_4$ for this experiment, we neglect the deexcitation terms and approximate equation (28) as follows.

$$W_4 = n_0 n_{Xe^+} L_0^4 + n_e n_1 S_1^4 \tag{29}$$

For the two 4d levels a similar expression for the pumping rate is obtained. However, for the two 4p levels only electron pumping is important so that assuming $S_1^2 = S_1^3$, we obtain

$$W_\ell = W_2 + W_3 = 2 n_e n_1 S_1^2 \tag{30}$$

Using equations (17a), (30), (29), and equations similar to (29) for the two 4d levels in equation (22) yields

$$R_{3968}^{3706} = 0.616 \frac{L_0^4 + N S_1^4}{A_{4\ell} \tau_\ell [N(B + 2S_1^2) + C]} \tag{31}$$

where,

$$B = S_1^4 + 2S_1^5 \tag{32a}$$

$$C = L_0^4 + L_0^5 + L_0^6 \tag{32b}$$

$$N = \frac{n_e n_1}{n_0 n_{Xe^+}} \tag{32c}$$

Since the two 4d levels are so close in energy we assumed that $S_1^5 = S_1^6$ in obtaining equation (31). The term B is the total electron excitation rate of the 5s and 4d levels while C is the total charge exchange rate for these same levels. For the electron temperatures of this

experiment $n_1/n_0 < 1$ and will increase with electron temperature. Also, since xenon ions are created in the plasma source where the electron temperature is highest we expect $n_{Xe^+} >> n_{Ca^+}$ so that for charge neutrality $n_{Xe^+} \approx n_e$. As a result, the density ratio term $N < 1$ and will increase with electron temperature, T_e.

In obtaining equation (31) we have assumed that both the 5s and 4d levels are populated by charge exchange with the same Xe^+ level (either the $^2P_{3/2}$ or $^2P_{1/2}$ level). It is possible that charge exchange with Xe^+ ($^2P_{3/2}$) may pump one level and charge exchange with Xe^+ ($^2P_{1/2}$) may pump the other level. If that were the case, then equation (31) would depend on the ratio of the Xe^+ ($^2P_{3/2}$) and Xe^+ ($^2P_{1/2}$) densities.

In interpreting the experimental intensity ratios we are interested in two limiting forms of equation (31). If charge exchange pumping of the 5s and 4d levels predominates over electron pumping of these levels then $NB << C$ and $NS_1^4 << L_0^4$ so that equation (31) becomes the following.

$$R_{3968}^{3706} = 0.616 \frac{L_0^4}{A_{4\ell}\tau_\ell(2NS_1^2 + C)} \qquad \text{Charge exchange pumping of 5s and 4d levels} \qquad (33)$$

The opposite limiting case is when electron pumping of the 5s and 4d levels is much larger than charge exchange pumping. In this case $NB >> C$ and $N_1S_1^4 >> L_0^4$ so that equation (31) becomes

$$R_{3968}^{3706} = 0.616 \frac{1}{A_{4\ell}\tau_\ell\left[1 + 2\left(\frac{S_1^2 + S_1^5}{S_1^4}\right)\right]} \qquad \text{Electron pumping of 5s and 4d levels} \qquad (34)$$

To determine how equations (33) and (34) vary with electron temperature, T_e, we must know how the electron excitation rates, S, and charge exchange excitation rates, L, depend on T_e. From reference 9 we obtain the following expression for the electron excitation rates:

$$S_i^j = C_i^j \left(\frac{q}{kT_e}\right)^{1/2} \exp\left(-\frac{qE_i^j}{kT_e}\right) \qquad (35)$$

where,

$$E_i^j = E_j - E_i \qquad (36)$$

is the energy difference between the j and i levels, k is the Boltzmann constant, and C_i^j is a constant. The electron excitation rate

given by equation (35) increases with T_e until $kT_e/q = 2E_i^j$ and then decreases for $kT_e/q > 2E_i^j$. The constant C_i^j has two different forms depending on whether the transition is allowed or forbidden.

For this experiment the relative velocity between the xenon ions and the calcium atoms, U, is much greater than the ion thermal speed. Also, the charge exchange cross section is nearly independent of U (see ref. 10). As a result the charge exchange rate can be approximated as,

$$L_0^i = U\sigma_0^i \tag{37}$$

where σ_0^i is the charge exchange cross section. Obviously, the charge exchange rate is independent of T_e.

Using equations (35) and (37) we can now determine how the intensity ratio for the two limiting conditions given by equations (33) and (34) depends on T_e. For the predominance of charge exchange pumping the T_e dependence of equation (33) is the following.

$$R_{3968}^{3706} \sim \frac{1}{2NC_1^2\left(\frac{q}{kT_e}\right)^{1/2} \exp\left(-\frac{qE_1^2}{kT_e}\right) + C} \qquad \text{Change exchange pumping of 5s and 4d levels} \tag{38}$$

From previous discussion we know that N is an increasing function of T_e. Also, since for this experiment $kT_e < 2qE_1^2$ the $(q/kT_e)^{1/2}$ $(q/kT_e)^{1/2} \exp[-qE_1^2/kT_e]$ term is also an increasing function of T_e. As a result, the intensity ratio, R_{3968}^{3706}, will be a decreasing function of T_e if charge exchange pumping of the 5s and 4d levels is much greater than electron pumping of these levels. If $C >> 2NS_1^2$ then R_{3968}^{3706} would be independent of T_e. The same conclusions apply to the R_{3934}^{3737}, R_{3968}^{3159}, R_{3934}^{3179}, and R_{3934}^{3181} intensity ratios.

Since $4p - 4s$ is an allowed transition while $4d - 4s$ is not allowed and also $E_1^5 \approx 2E_1^2$, S_1^5 can be neglected in equation (34). Therefore, using equation (35) in (34) we find the T_e dependence of R_{3968}^{3706} in the case where electron pumping predominates over charge exchange is the following.

$$R_{3968}^{3706} \sim \frac{1}{1 + \frac{2C_1^2}{C_1^4} \exp\left(\frac{qE_2^4}{kT_e}\right)} \qquad \text{Electron pumping of 5s and 4d levels} \tag{39}$$

Therefore, R_{3968}^{3706} will be an increasing function of T_e if electron pumping of the 5s and 4d levels is much greater than charge exchange pumping of these levels. The same conclusion applies to the R_{3934}^{3737}, R_{3968}^{3159}, R_{3934}^{3179}, and R_{3934}^{3181} intensity ratios.

There are two additional intensity ratios that will be used in analyzing the experimental data. From equations (18a), (18b), (26), (27), and (37) the following results are obtained if charge exchange is the pumping mechanism for the 5s and 4d levels.

$$R_{3706}^{3159} = 4.26 \frac{A_{4\ell}}{A_{5\ell}} \frac{\sigma_0^5}{\sigma_0^4} \tag{40a}$$

$$R_{3159}^{3179} = 1.17 \frac{A_{5\ell}}{A_{63}} \frac{\sigma_0^6}{\sigma_0^5} \tag{40b}$$

Charge exchange pumping of 5s and 4d levels

For electron pumping of the 5s and 4d levels these same intensity ratios are obtained by using equations (18a), (18b), (26), (27), and (35).

$$R_{3706}^{3159} = \frac{C_{15}}{C_{14}} \exp\left(-\frac{qE_4^5}{kT_e}\right) \tag{41a}$$

$$R_{3159}^{3179} = \frac{C_{16}}{C_{15}} \exp\left(-\frac{qE_5^6}{kT_e}\right) \approx \frac{C_{16}}{C_{15}} \tag{41b}$$

Electron pumping of 5s and 4d levels

EXPERIMENTAL RESULTS

Experimental Apparatus

Figure 1 is a schematic diagram of the experimental apparatus. The lower power, steady state MPD arc operates at voltages less than 100 volt and currents up to 5 amps. The velocity of the plasma in the exhaust is the order of 10^6 cm/sec. A 0.318 cm diameter thoriated tungsten rod with a 0.235 cm diameter hole drilled in it and with a 0.0375 cm diameter orifice plate serves as the hollow cathode. The cylindrical stainless steel anode has an edge wound electromagnet around it. A magnetic field of approximately 0.015 tesla at the cathode tip was used for the experiment. The flow rate of xenon was approximately 3×10^{-3} gm/sec.

Relative intensity measurements were made with 1/2 m scanning monochromator. The monochromator viewed the plasma through a quartz window in the region where calcium was injected. Calcium entered the plasma by sublimation from a calcium ribbon. The calcium ribbon was wrapped around a nichrome wire which was resistively heated to calcium sublimation temperatures. The amount of calcium being injected could be varied by changing the power input to the nichrome wire. Varying the amount of calcium injection had negligible effect on the intensity ratios to be discussed below.

A double Langmuir probe was used to measure the plasma electron

density and temperature. The design of the probe is described in reference 7. When the double probe was used in the calcium seeded plasma it was quickly contaminated so that reliable probe current versus probe voltage data could not be obtained. As a result probe data were taken only when calcium was not present.

Results

Figure 3 shows the electron temperature increasing with power input to the plasma source. As pointed out earlier, the double Langmuir probe became contaminated in the Ca-Xe plasma. Therefore, the electron temperature as a function of power input shown in figure 3 is for a Xe plasma only. With the addition of calcium I expect only the magnitude of T_e to change and not the shape of the T_e versus power input curve. As a result, I conclude that T_e is an increasing function of power input for the Ca-Xe plasma.

The intensity ratios (shown in figs. 4(a) and (b)) are monotonically decreasing functions of power input. Based on the results of figure 3, I then conclude that these intensity ratios are also monotonically decreasing functions of T_e. As discussed earlier (see eq. (38)), this is the electron temperature dependence expected if charge exchange is the predominate pumping mechanism for the 5s and 4d levels of Ca^+.

The intensity ratios that indicate the density of the 5s level (fig. 4(b)) are very nearly independent of T_e. This has two possible explanations. Either charge exchange pumping is much greater than electron pumping of all levels (see eq. (38)) or electron collisions, which are neglected in equation (38), are contributing a significant amount to the population of the 5s level. The intensity ratio R_{3934}^{3181} is not shown in figure 4 because the intensity for the $\lambda = 3181$ transition was so low that reliable data could not be obtained.

Comparing an estimate of the magnitude of R_{3968}^{3706} obtained from equation (34) with the experimental result indicates that electron collisions alone cannot account for the pumping of the 5s level. The energy of the 4p levels is less than one half the energy of the 5s and 4d levels. Also, transitions from the 5s and 4d levels to the ground state are not allowed while the 4p to ground state transitions are allowed. As a result the electron excitation rate of the 4p levels, S_1^2, will be larger than the excitation rate of the 5s and 4d levels, S_1^4 and S_1^5 (see eq. (34)), assume $S_1^2 \approx S_1^4 \approx S_1^5$. Also, from figure 2 we obtain $A_{4\ell} = A_{42} + A_{43} = 2.49\times10^8 \text{ sec}^{-1}$ and $\frac{1}{\tau_\ell} = A_{21} + \frac{g_2}{g_3} A_{31} = 2.21\times10^8 \text{ sec}^{-1}$. Using these values in equation (34) we obtain $R_{3968}^{3706} \approx 0.11$. From figure 4(b) we see that $R_{3968}^{3706} > 0.11$ for all the data points. Similar results can be obtained by comparing estimates of R_{3934}^{3737}, R_{3934}^{3179}, and R_{3698}^{3159} with measured values of these intensities.

Further evidence to indicate that charge exchange between Xe^+ and Ca is responsible for populating the 5s and 4d levels is given in Table I. Here results obtained with Ca-Ar and Ca-Kr are compared with the Ca-Xe results. The Ca-Xe results at power input of 160 watts were obtained by extrapolating the results of figure 4. Since neither Ar^+ nor Kr^+ has a near resonance with the 5s or 4d levels of Ca^+ we do not expect charge exchange to pump the 5s or 4d levels in the Ca-Ar or Ca-Kr systems. If electron collisions are the predominate pumping mechanism for these levels then the results in Ar should show the largest intensity ratios since we expect Ar to have the largest T_e because of its large ionization potential. Since Xe has the lowest ionization potential we expect it to have the lowest T_e. As a result the intensity ratios in Ca-Xe should be the smallest if electron collisions do the pumping of the 5s and 4d levels. Table I results show that the intensity ratios are largest in Ca-Xe. One may conclude again that electron collisions cannot be the predominate mechanism for pumping the 5s and 4d levels in the Ca-Xe system.

Figure 5 shows the intensity ratio R_{3706}^{3159} as a function of input power. Since R_{3706}^{3159} shows no recognizable trend with power input we conclude that it is independent of electron temperature. An average value, R_{3706}^{3159}, for the power range 55 to 145 watts is 2.48. This is the expected result if charge exchange is the populating mechanism for the 5s and 4d levels (see eq. (40a)). A similar conclusion results from the data for the intensity ratios R_{3737}^{3159}, R_{3706}^{3179}, R_{3737}^{3179}. Using average values for these ratios we can calculate the cross section ratios σ_0^5/σ_0^4 and σ_0^6/σ_0^4. These results are shown in table II. In all cases $\sigma_0^5/\sigma_0^4 < 1$ and $\sigma_0^6/\sigma_0^4 < 1$. This implies that charge exchange pumping of the 5s level is more probable than charge exchange pumping of the 4d levels. It should be remembered, however, that we have assumed charge exchange with the same Xe^+ level has been responsible for populating both the 5s and 4d levels. If charge exchange with Xe^+ ($^2P_{1/2}$) pumps the 4d levels and charge exchange with ground state Xe^+ ($^2P_{3/2}$) pumps the 5s level then the values in table II should be multiplied by the ratio of the Xe^+ ($^2P_{3/2}$) density to the Xe^+ ($^2P_{1/2}$) density. This ratio is greater than one so that it is possible that $\sigma_0^5/\sigma_0^4 > 1$ and $\sigma_0^6/\sigma_0^4 > 1$.

The intensity ratio R_{3159}^{3179} was also found to have no noticeable trend with power input. Such a result is expected for either electron collisional or charge exchange pumping of the 4d levels (see eq. (40b)). An average value of $R_{3159}^{3179} = 1.35$ was obtained. Using R_{3159}^{3179} in equation (27) yields the following.

$$\frac{n_6}{n_5} = 1.15 \tag{42}$$

If the $4d\,^2D_{3/2}$ and $4d\,^2D_{5/3}$ levels are in equilibrium we expect the following results.

$$\left(\frac{n_6}{n_5}\right)_{eq} = \frac{g_6}{g_5} e^{-qE_5^6/kT_e} \approx \frac{g_6}{g_5} = 1.5 \tag{43}$$

Comparing equations (42) and (43) we conclude that the $4d^2D_{3/2}$ and $4d^2D_{5/2}$ are not in equilibrium. Using $R_{3159}^{3179} = 1.35$ in equation (40b) we obtain

$$\frac{\sigma_0^6}{\sigma_0^5} = 1.13 \tag{44}$$

Therefore, the $J = 5/2$ level has a larger charge exchange cross section than the $J = 3/2$ level.

The energy difference between the $4d^2D_{3/2}$ and the $4d^2D_{5/2}$ levels is less than 0.003 eV. Therefore, we expect each of the states of the $J = 3/2$ and $J = 5/2$ levels has the same probability of being populated by charge exchange. As a result, the ratio given by equation (44) should equal the ratio of the statistical weights. For this case the ratio of statistical weights is 1.5, so there is fairly good agreement between this result and equation (44). Melius[4] points out that for larger energy differences the ratio of the cross sections should be larger than the ratio of the statistical weights. Experimental results[5] in He-Zn for the $6p^2P_{3/2}$ and $6p^2P_{1/2}$ levels of Zn^+ (energy difference = 0.009 eV) yield a cross section ratio of 7.5. The ratio of the statistical weights for these levels is 2. For the $5d^2D_{5/2}$ and $5d^2D_{3/2}$ levels the energy difference is only 0.003 eV and the experimental result[5] for the cross section ratio is 1.8. This agrees fairly well with the statistical weight ratio of 1.5.

As expected, the intensity ratio R_{3968}^{3934} was also independent of input power. An average value $R_{3968}^{3934} = 2.11$ was obtained. From equation (21),

$$R_{3968}^{3934} = \left(\frac{3968}{3934}\right) \frac{A_{31}}{A_{21}} \frac{n_3}{n_2} \tag{45}$$

Using $R_{3968}^{3934} = 2.11$ and the transition probabilities shown in figure 2 we obtain the following.

$$\frac{n_3}{n_2} = 2.03 \tag{46}$$

This result is very close to the equilibrium result that was used in deriving equations (17a) to (17c). For equilibrium

$$\left(\frac{n_3}{n_2}\right)_{eq} = \frac{g_3}{g_2} e^{-qE_2^3/kT_e} \approx \frac{g_3}{g_2} = 2 \qquad (47)$$

We therefore conclude that it is valid to assume the $4p^2P_{1/2}$ and $4p^2P_{3/2}$ levels are in equilibrium.

CONCLUSION

Three pieces of evidence indicate that charge exchange between Xe^+ and Ca is the predominate mechanism for populating the 5s and 4d levels of Ca^+.

1. Intensity ratios that are proportional to the ratios of the 5s to 4p and 4d to 4p level densities are decreasing functions of electron temperature. This is the expected result if charge exchange is the pumping mechanism. If electron collisions were the pumping mechanism, then the intensity ratios would be increasing functions of electron temperature.

2. The intensity ratios described above were also measured in Ca-Ar and Ca-Kr. Values in Ca-Xe were 2 to 10 times greater than in Ca-Ar and Ca-Kr. If electron collisions were the pumping mechanism, the Ca-Xe intensity ratios would be expected to be the lowest.

3. Intensity ratios that are proportional to the ratios of the 4d to 5s level densities are independent of electron temperature. This is the expected result for charge exchange pumping of the 5s and 4d levels.

REFERENCES

1. D. L. Chubb and J. R. Rose, Appl. Phys. Lett. 22, 417 (1973).

2. H. S. W. Massey and E. H. S. Burhop, Electronic and Ionic Impact Phenomena (Clarendon Press, Oxford, 1952) Chap S. VII and VIII.

3. E. W. McDaniel, Collision Phenomena in Ionized Gases (John Wiley & Sons, New York, 1964) p. 240.

4. Melius, C. F.; to be published.

5. A. R. Turner-Smith, J. M. Green, and C. W. Webb, J. Phys. B 6,114 (1973).

6. G. R. Seikel, D. J. Connolly, C. J. Michels, E. A. Richley, J J. M. Smith, and R. J. Sovie, in Plasmas and Magnetic Fields in Propulsion and Power Research, NASA SP-226 (1970) p. 1.

7. D. L. Chubb, NASA TN D-7223, 1973.

8. W. L. Wiese M. W. Smith, and B. M. Miles, National Bureau of Standards Report NSRDS-NBS 22 (1968), p. 251.

9. R. C. Elton, in Methods of Experimental Physics Plasma Physics, Vol. 9A edited by H. R. Griem and R. H. Lovberg (Academic Press, New York, 1970) p. 115.

10. D. L. Chubb and J. R. Rose, NASA TM X-68143, 1972.

TABLE I. - COMPARISON OF CALCIUM ION INTENSITY RATIOS IN ARGON, KRYPTON, AND XENON

Gas	R_{3968}^{3159}	R_{3934}^{3179}	R_{3968}^{3706}	R_{3934}^{3737}	Input power, watt
Argon	0.056	0.012	0.055	0.057	160
Krypton	0.0324	0.026	0.039	0.032	132
Xenon	0.32	0.14	0.11	0.11	160

TABLE II. - CHARGE EXCHANGE CROSS SECTION RATIOS

Transition ratio	Average intensity ratio	Cross section ratio
$\frac{4d^2D_{5/2} \rightarrow 4p^2P_{3/2}}{5s^2S_{1/2} \rightarrow 4p^2P_{3/2}}$	$R_{3737}^{3179} = 1.5$	$\frac{\sigma_0^6}{\sigma_0^4} = 0.85$
$\frac{4d^2D_{5/2} \rightarrow 4p^2P_{3/2}}{5s^2S_{1/2} \rightarrow 4p^2P_{1/2}}$	$R_{3706}^{3179} = 3.3$	$\frac{\sigma_0^6}{\sigma_0^4} = 0.96$
$\frac{4d^2D_{3/2} \rightarrow 4p^2P_{1/2}}{5s^2S_{1/2} \rightarrow 4p^2P_{1/2}}$	$R_{3706}^{3159} = 2.5$	$\frac{\sigma_0^5}{\sigma_0^4} = 0.85$
$\frac{4d^2D_{3/2} \rightarrow 4p^2P_{1/2}}{5s^2S_{1/2} \rightarrow 4p^2P_{3/2}}$	$R_{3706}^{3159} = 1.1$	$\frac{\sigma_0^5}{\sigma_0^4} = 0.75$

Superscripts:

4 - Ca^+ ($5s^2S_{1/2}$)

5 - Ca^+ ($4d^2D_{3/2}$)

6 - Ca^+ ($4d^2D_{5/2}$)

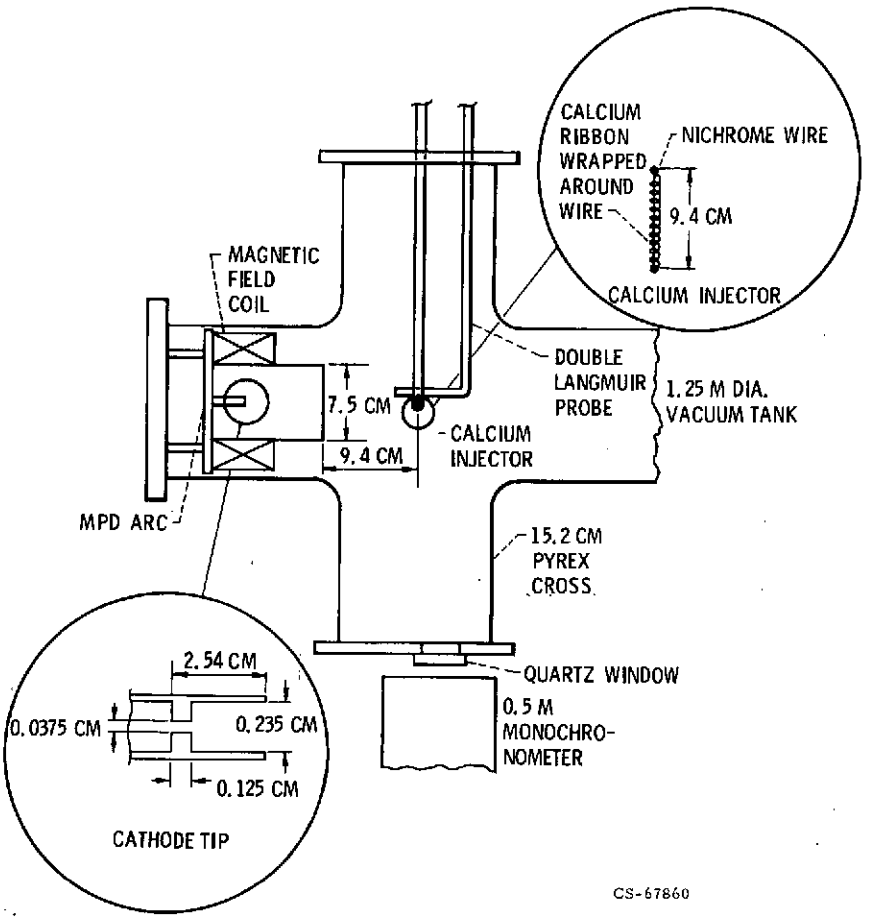

Figure 1. - Experimental apparatus.

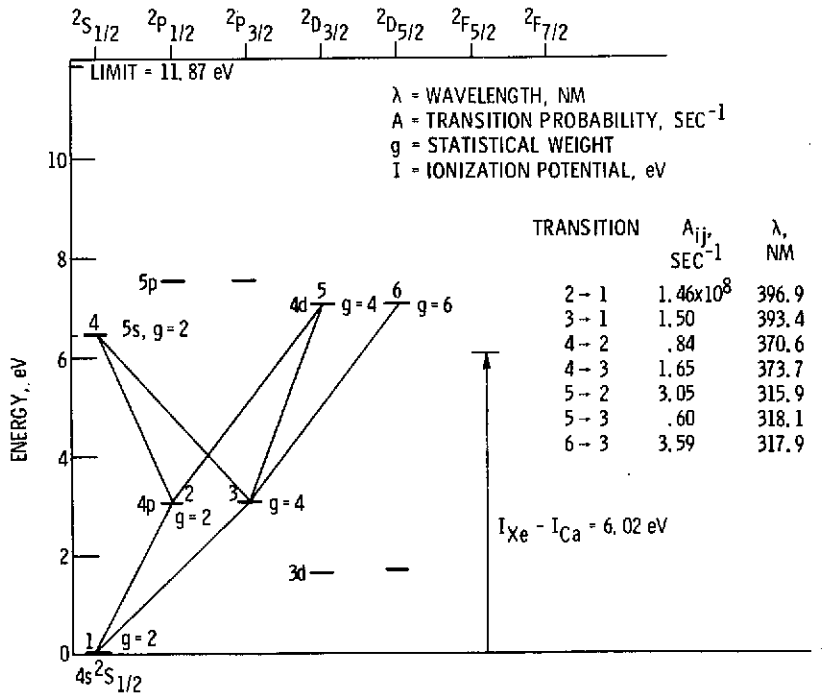

Figure 2. - Energy level diagram for calcium ion.

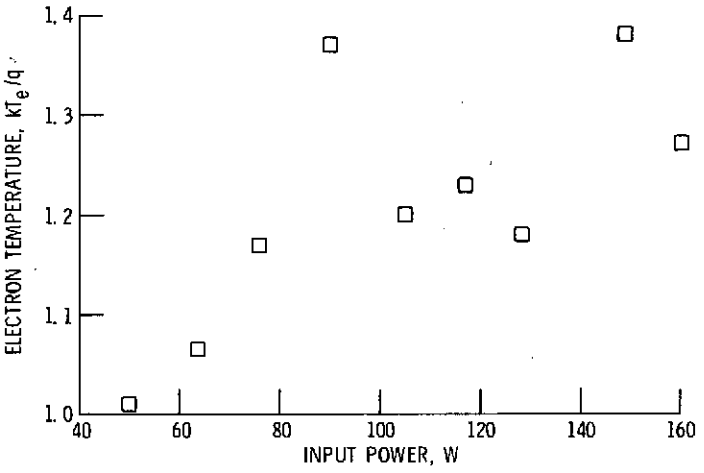

Figure 3. - Electron temperature versus power input (no calium seed).

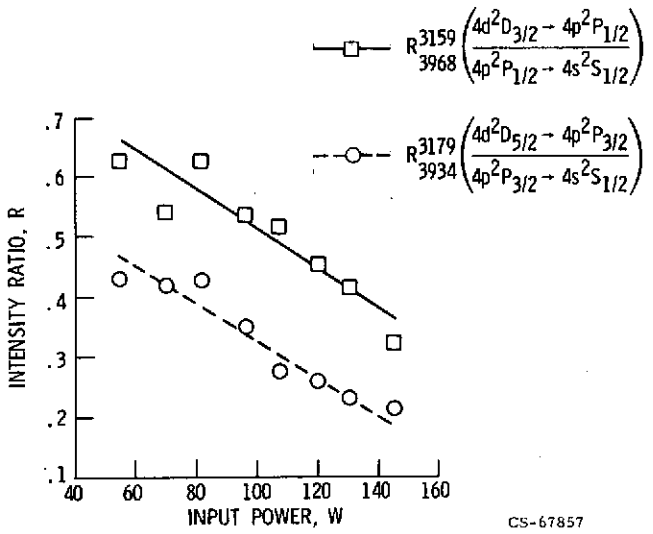

(A) INTENSITY RATIOS FOR 4d→4p/4p→4s TRANSITIONS.

Figure 4. - Intensity ratios versus power input.

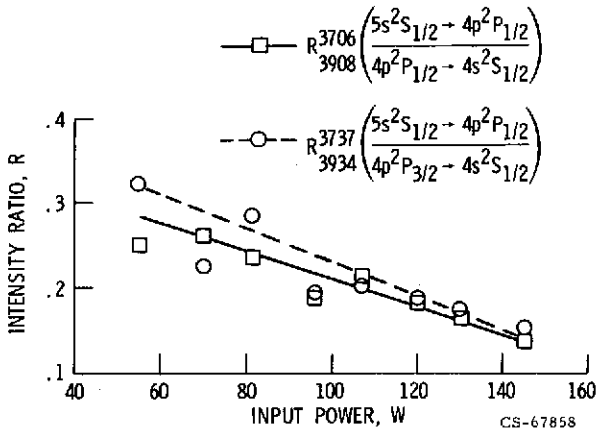

(B) INTENSITY RATIOS FOR 5s→4p/4p→4s TRANSITIONS.

Figure 4. - Concluded.

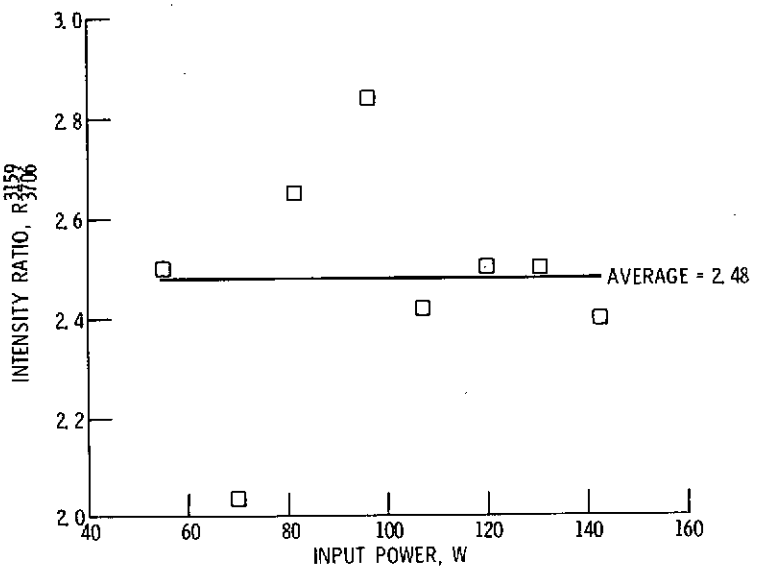

Figure 5. - Intensity ratio for $4d^2D_{3/2} \rightarrow 4p^2P_{1/2}/5s^2S_{1/2} \rightarrow 4p^2P_{1/2}$ transition versus power input.